(2)

Interface states and electron spin resonance centers in thermally oxidized (111) and (100) silicon wafers

Edward H. Poindexter and Philip J. Caplan
U. S. Army Electronics Technology and Devices Laboratory, Fort Monmouth, New Jersey 07703

Bruce E. Deal and Reda R. Razouk
Research and Development Laboratory, Fairchild Camera and Instrument Corporation, Palo Alto, California 94304

DTIC ELECTE APR 13 1983 S D

(Received 22 July 1980; accepted for publication 6 October 1980)

Interface states and electron spin resonance centers have been observed and compared in thermally oxidized (111) and (100) silicon wafers subjected to various processing treatments. The ESR P_b signal, previously assigned to interface $\cdot Si{\equiv}Si_3$ defects on (111) wafers, was found to have two components on (100): an $\cdot Si{\equiv}Si_3$ center oriented in accord with (100) face structure, and an unidentified center consistent with $\cdot Si{\equiv}Si_2O$. The quantitative proportionality of P_b spin concentration to midgap interface trap density D_{it} is maintained on (100), and both are lower by a factor of about 3 compared to (111). This correlation persists over the range of oxidation temperatures 800–1200°C, for both *n*- and *p*-doped silicon, cooled by fast pull in oxygen, and cooled or annealed in nitrogen or argon. The correlation is independent of doping level. In samples with different oxide thickness, neither P_b nor D_{it} varied significantly over the range 100–2000 A, but P_b was smaller at 50 A. In general, ESR is judged to offer promise for further studies of specific interface features.

PACS numbers: 73.40.Qv

AD A126719

INTRODUCTION

The technological thrust toward silicon integrated circuits with micrometer and submicrometer elements has emphasized the need for an improved structural model of the critical Si/SiO_2 interface in thermally oxidized wafers.[1] In addition, new analytical techniques which respond to important features of integrated circuit (IC) materials, e.g., defects, would be of considerable help in developing better processing methods. Our previous studies have shown that electron spin resonance (ESR) can be useful in both areas.[2]

In the earlier work metal-oxide-semiconductor test structures were fabricated with a selected variety of material and process parameters. These parameters included silicon substrate orientation and dopant type, dry O_2 oxidation temperature, and annealing/cooling conditions. Some experiments using H_2O and O_2-HCl oxidizing ambients were also conducted. Numerous samples were examined by *C-V* electrical analysis, as well as by ESR. This earlier study was largely confined to (111) wafers, owing to ESR sensitivity limitations. The primary ESR signal of interest, termed P_b,[3] was assigned to oriented trivalent silicon atoms at the interface in the $\cdot Si{\equiv}Si_3$ configuration. A fairly good quantitative correlation between P_b concentration and midgap interface state density D_{it},[4] was observed after the various processing treatments.

In the second phase of the study, reported here, additional processing variables, such as high-temperature *in situ* anneal ambients, and their effects on oxide charges were examined. The effect of oxide thickness variations on the concentration of trapped charges and intensities of ESR signals was investigated. The effects of dopant variations (type and concentration) were included. Analysis of the P_b signal was extended to (100) wafers, which are more common for device applications, so that any differences between (100) and (111) oxide interfaces could be contrasted. Comparisons between the results of ESR and *C-V* measurements were limited to the $P_b - D_{it}$ relationship, since earlier inconsistent evidence of $P_b - N_f$,[4] correlation[2] appeared to be confined to cases where D_{it} and N_f were also correlated.

DTIC FILE COPY

EXPERIMENTAL CONSIDERATIONS

A comprehensive discussion of wafer sample preparation and basic *C-V* and ESR procedures has been presented previously.[2] Unless otherwise stated, samples for *C-V* study were *n*- and *p*-type 4–6 Ω cm silicon wafers; samples for ESR measurements were wafer slices, cut 4×20 mm, *n*- and *p*-type, 100 Ω cm or greater. ESR spectra were usually observed at 295°K. Essential details and modifications for the different investigations will be given in the appropriate section.

An improved ESR technique was required for this extended study. The P_b signals from (100) wafers are inherently nearly an order of magnitude weaker than (111) for two reasons: the density of spin centers is about one-third that of (111), and the signal is split into components. In the previous study, very crude results were obtained. For the present work, wafer-slicing alignment was held within 1°. The samples were suspended in the cavity by tested non-resonant fibers without silica or Vycor tubes, and a laser was used for improved positioning inside the cavity. For the *g*-tensor study, samples with a (100) face were cut with (011) long side. The sample was rotated about the (011) axis with the magnetic field H_0 lying in the (011) plane. The rotation angle was 90° in steps of 7.5° from 0°, with H_0 along the (100) face axis, through (111), to 90° with H_0 along the (011) axis. Although the observed *g*-tensor is completely defined by this 90° rotation, some confirming spectra were observed outside this range.

 0021-8979/81/020879-06$01.10 © 1981 American Institute of Physics

83 04 12 087

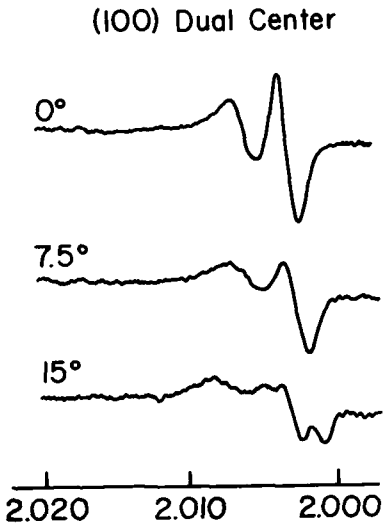

FIG. 1. Selected ESR signals from interface P_b centers in thermally oxidized (100) silicon wafers. Magnetic field H_0 lies in the (011) rotation plane and is normal to (100) at 0° rotation.

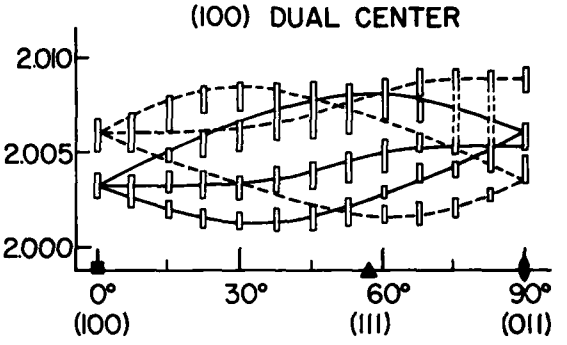

FIG. 2. ESR g-value anisotropy map for P_b centers on (100) silicon. The two centers P_{b0} and P_{b1} are respectively indicated by dashed and solid lines. Rotation plane (011).

RESULTS AND DISCUSSION

2. Nature of EST P_0 centers on (100) wafers

Of all the ESR centers observed in Si wafers, only the P_b center appears to have an essential connection with the inherent structure of the uncontaminated Si/SiO_2 interface. It therefore merits special study and discussion, whereas other centers,[3,5,6] P_a, P_c, D, and E' occur less generally; and though found near the interface, they occur in bulk regions. Of these latter four, only P_a will be discussed briefly in concert with other experimental features in a later section.

A selection of the observed anisotropic (100) P_b signals is shown in Fig. 1. Comparison with our earlier work[2] shows the present much better signal-to-noise ratio. The signal is resolved into two, three, or four components, depending on rotation angle of the wafer in the field. This signal anisotropy has one very important meaning even without further analysis: it indicates that the P_b signal is definitely responding to interface crystallography. This dashes any possibility that the g-tensor anisotropy of the P_b center on (111) wafers might be due to its interface location, rather than crystal structure.

The anisotropy map for P_b (100) is shown in Fig. 2. The most readily fitted resolution of the total pattern requires contributions from two distinct ESR centers, distinguished by dashed and solid lines in the plot. These two centers will be called P_{b0} and P_{b1}, respectively; and the deduced values for the g-tensors, along with values for P_b from (111) wafers, are summarized in Table I. The identical lattice orientations of g-tensors for P_{b_0} (100) and P_b (111) and the near equality of respective g-values strongly suggest the identity of these two species. Thus P_{b0} (100) is reasonably assigned to $\cdot Si{\equiv}Si_3$ on the (100) face. The Si^{III} unbonded orbital on (100) wafers is inclined to the wafer face in accord with apparently near-perfect interface Si crystal structure, analogous to the perpendicular Si^{III} orbital position on (111) wafers.

The second component of the (100) center, P_{b1} has a triaxial g tensor which is not like any of the numerous centers in either Si or SiO_2 analyzed elsewhere.[7,8] In respect to crystal symmetry, P_{b1} is consistent with $\cdot Si{\equiv}Si_2O$ centers. Because of the limited evidence available at this time, this assignment is tentative.

The dual P_b (100) center was examined in a number of different sets of sample wafers, in order to seek possible distinction of P_{b0} and P_{b1} with different annealing procedures. While no consistent chemical effect could be determined, some wafers did show a much different balance of P_{b0} to P_{b1}. Not only did this facilitate more confident resolution of the g-anisotropy map, it also suggests a means for monitoring subtle interface chemistry. Figure 3 shows a few ESR signals which have a simpler structure than those in Fig. 1. Figure 4 shows the anisotropy map for this second set of wafers, illustrating the result of the much-reduced P_{b0} signal. The separate identity of P_{b1} is thus confirmed.

A model of the Si/SiO_2 interface on (100) silicon derived from these ESR results is shown in Fig. 5. The more well-established $\cdot Si{\equiv}Si_3$ center is shown with two different orientations. The speculative $\cdot Si{\equiv}Si_2O$ center is also indicated. It is apparent from the figure that it is fairly easy to derive the latter center as a natural part of the advancing oxide front; no awkward oxygen "scouts", inserted well into the silicon,

TABLE I. ESR g values for P_b centers in oxidized (111) and (100) silicon wafers. Principal values are observed along the specified crystal axes. The value with H_0 normal to the wafer face is denoted g_f. Note that interface defects are constrained to fewer lattice orientations than bulk defects.

	(100)	$\cdot Si{\equiv}Si_3$	(100)	$\cdot Si{\equiv}Si_2O(?)$	(111)	$\cdot Si{\equiv}Si_3$
g_f	2.0060	∥(100) axis	2.0032	∥(100) axis	2.0013	∥(111) axis
g_1	2.0015	approx.∥(111) axis	2.0012	between (100), (111) axes	2.0013	∥(111) axis
g_2	2.0080	between (100), (111) axes	2.0076	approx. ∥(111) axis	2.0086	rot. symm.
g_3	2.0087	∥(011) axis	2.0052	∥(011) axis	2.0086	rot. symm.

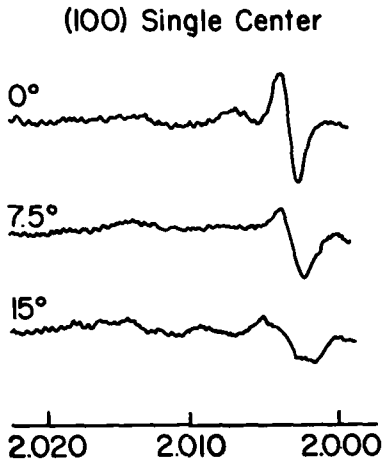

FIG. 3. P_b signals from (100) wafers, showing the effects of diminution of one of the two centers contributing to the total P_b signal.

are required. In contrast, an analogous partially oxidized structure is much more difficult to envision on (111). This may explain the simple defect structure of the (111) face. The other ESR defects considered[2] on (111) are not portrayed in Fig. 5. However, ESR of the (100) interface is clearly dominated by the two P_b species, with other possible centers playing a lesser role.

B. Oxide charges and ESR for wafers oxidized and cooled in dry O_2

Process variations such as annealing and cooling are known to play a substantial role in determining the concentration of oxide charges and have been discussed in detail elsewhere.[1,9,10] These variations were observed to have strong effects on ESR signals as well. It was also noted that the relationship between P_b centers and D_{it} was affected in some cases. Figure 6 illustrates the relationship obtained in this study for sample oxidized in dry O_2 at various tempertures and cooled by fast pull in O_2 [O_2 (FP)]. Both (100) and (111) samples, *n*- and *p*-type, are shown; and although scatter is evident in the data, a quantitative correlation seems to exist between the ESR data and the midgap values of D_{it} as measured by the quasistatic technique. This correlation persists thoughout the range of oxidation temperatures, 800–1200°C. The concentration of ESR centers is approximately

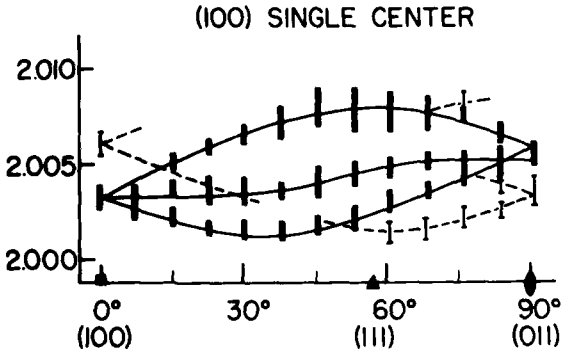

FIG. 4. ESR *g*-value anisotropy of P_b on (100) wafers with diminished $\cdot Si \equiv Si_3$ centers. Rotation plane (0$\bar{1}$1).

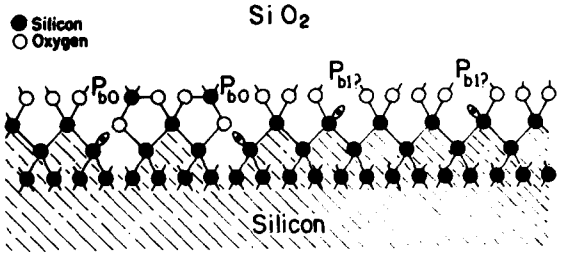

FIG. 5. Structural model of the (100) Si-SiO_2 interface in accord with ESR analysis.

equal to the midgap interface state density for both (100) and (111) wafers, and a ratio of about 1:3 between (100) and (111) holds for both D_{it} and P_b. The ratio D_{it}:P_b is about the same for *n*- and *p*- type samples, although both quantities are lower in *p*-type. The apparent finite intercept along the D_{it} axis is in accord with the idea that P_b centers might be associated with some, but not all interface states.

C. Effect of inert gas anneals on D_{it} and P_b

The annealing of thermally grown silicon dioxide films in inert ambients, particularly nitrogen, has been used extensively in integrated circuit fabrication. Often the anneal is carried out *in situ* at the oxidizing temperature. Such anneals can effect a reduction in charge densities, particularly for anneals around 1000°C and for oxide thickness greater than 1000 A. Differences have, however, been reported between annealing in nitrogen and in argon with respect to the resulting oxide charges;[1] and a reaction betweeen nitrogen and the silicon substrate has been proposed.[11,12]

In the experiments reported here, wafers were oxidized at 1000 or 1200°C for 360 or 60 min, respectively, and subsequently annealed *in situ* in nitrogen or argon for 10 or 60 min at the oxidizing temperature. Typical interface state density distributions for both nitrogen and argon are shown in Fig. 7 for *n*- type (100) samples oxidized and annealed at 1200°C;

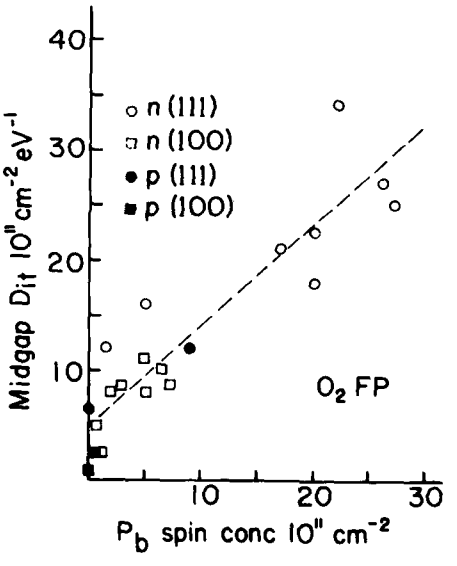

FIG. 6. Correlation of P_b concentration and midgap D_{it} on oxidized silicon wafers cooled by fast pull in dry O_2.

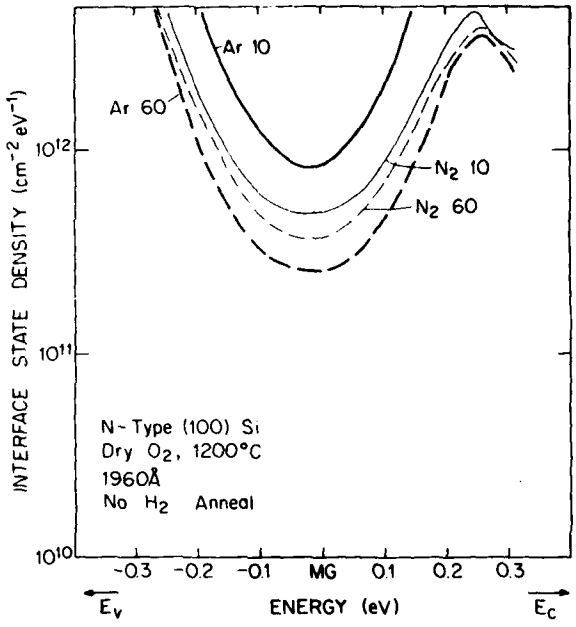

FIG. 7. Interface state density distribution for n-type (100) silicon oxidized in dry O_2 at 1200°C and annealed *in situ* for 10 or 60 min. in N_2 or Ar.

they indicate a basic similarity in both magnitude and energy distribution for wafers annealed in either gas. Characteristic of the measurements are a steeply rising peak of interface states above midgap (0.2-0.3eV below the conduction band), a minimum around midgap, and a high level of interface states (probably a peak) below midgap. Similar results were obtained on p-type (100) samples, showing a definite peak below midgap of smaller magnitude than for n- type wafers. The D_{it} values obtained from quasistatic measurements on this set of p-type wafers were generally lower than values obtained on the corresponding n-type wafers.

The correlation betweeen the P_b signal and D_{it} for nitrogen anneals has been separated by dopant type in Fig. 8.

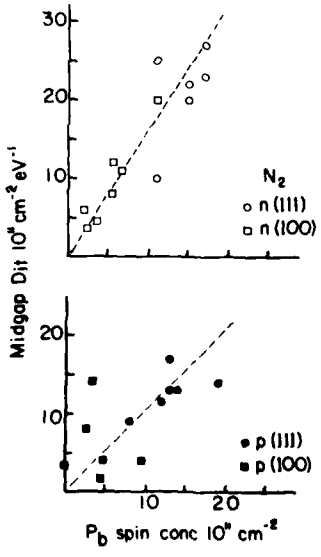

FIG. 8. Comparison of P_b – D_{it} relationship in oxidized n- and p-type silicon wafers cooled or annealed in nitrogen.

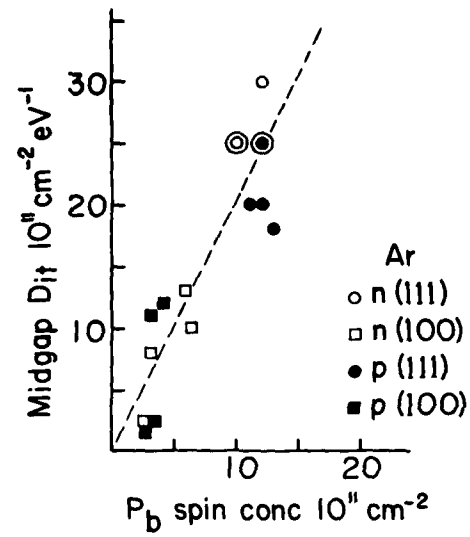

FIG. 9. Correlation of P_b and D_{it} in oxidized silicon wafers cooled or annealed in argon.

The plots look different and have different D_{it} vs P_b slopes. The cause of these differences is not clear at this time, although they may reflect a more complex interface chemistry and a delicate quasi-equilibrium in N_2-annealed wafers.

For argon-annealed wafers a higher level of interface states was observed with short anneal time (10 min) and a lower level for longer anneal time (60 min) as compared to nitrogen-annealed samples for 10 and 60 min, respectively. Prolonged anneal times in either gas seemed to reduce "as-oxidized" interface states at 1000 and 1200°C while increasing fixed oxide charge density at 1200°C. The correlation between P_b and D_{it} for argon-annealed wafers is shown in Fig. 9. There was apparently no difference between n-type and p-type wafers, and they are plotted together.

D. Oxide thickness variations

The effects of oxide thickness on interface states D_{it} and P_b centers were investigated. The samples were oxidized in dry O_2 at 1000°C for times ranging from 2 min to 6 hr. The

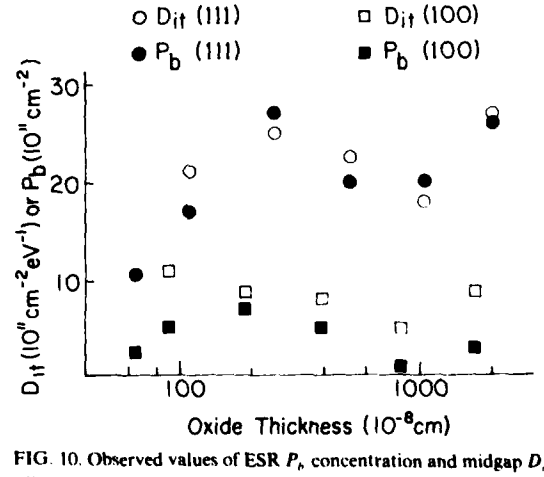

FIG. 10. Observed values of ESR P_b concentration and midgap D_{it} for silicon wafers with different oxide thickness. Wafers oxidized in dry O_2 at 1000°C for 2 min to 6 h, and pulled from oxidizing ambient in < 3 sec.

resulting oxide thicknesses ranged from 50 to 2010 A. Following oxidation the wafers were pulled from the oxidizing ambient in less than 3 sec (FP). Electrical C-V analysis was possible only at 100 A and above, due to pinhole problems. ESR spectra were obtainable even on the 50-A oxides. ESR data were taken at nonsaturating power levels; an easier saturability was noted in thicker oxides.

The observed data are presented in Fig. 10. Midgap values of D_{it} for (111) wafers ranged from 18×10^{11} to 27×10^{11} $cm^{-2}\,eV^{-1}$, with no particular trend discernible. For (100) wafers, D_{it} ranged from 5 to 11×10^{11} $cm^{-2}\,eV.^{-1}$ Corresponding ranges for P_b centers were 17 to 27×10^{11} spin cm^{-2} for (111), and 1 to 7×10^{11} spin cm^{-2} for (100). There was a virtually 1:1 quantitative correlation between P_b and N_{it} for the (111) wafers over the thickness range 100–2000 A. At 50 A, P_b fell by a factor of 2. The correlation between P_b and D_{it} was only semiquantitative for (100) wafers, with a D_{it} averaging about twice P_b. Both D_{it} and P_b are 3 to 5 times weaker on (100) as compared to (111) wafers.

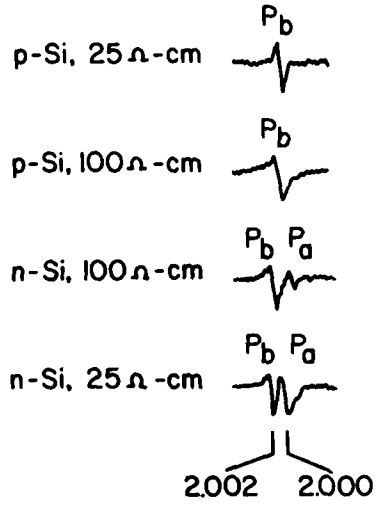

FIG. 11. ESR signals in oxidized n- and p-type (111) silicon, showing emergence of P_a signal in n-doped wafers.

E. Dopant concentration variations

The investigation of the effects of variations in dopant type and concentration on ESR signals and oxide charges was carried out by using p- and n- type (111) wafers of resistivity 25, 50, and 100 Ω-cm. The wafers were oxidized at 1000°C for 360 min in dry O_2 and cooled in either nitrogen or oxygen. The first significant aspect of this experiment rests in the fact that D_{it} and P_b throughout this program have usually been measured on separate samples of silicon having different resistivities. This was done to operate in the region most suitable for each measurement technique. Effects due to dopants, particularly as they relate to ESR measurements, are therefore necessary to get a complete picture of the process dependence of D_{it} and P_b, and their relationship to each other. The second objective of this set of experiments was the direct comparison of ESR and D_{it} results on identical specimens, for a more realistic correlation.

No observable dopant concentration effects were noted on oxide charges in this doping range. Before hydrogen annealing, midgap D_{it} was 33 ± 4 (10^{11} $cm^{-2}\,eV^{-1}$) for oxygen pulls, and 21 ± 3 (10^{11} $cm^{-2}\,eV^{-1}$) for nitrogen. ESR signals likewise showed no dopant concentration effects. For oxygen pulls, P_b concentration was 14 ± 1 (10^{11} spin cm^{-2}), and for nitrogen, 10 ± 1 (10^{11} spin cm^{-2}). In this case, the average ratio of midgap D_{it} to P_b concentration is a little more than 2:1. There is no reason to expect identical values for D_{it} and P_b even if P_b were a source of all interface states. Our midgap D_{it} values are deconvolved from the swept-voltage C-V curve; the observed P_b signal, however, arises only from those spin levels occupied by a single electron under zero-bias band-bending conditions.

In addition to the invariant P_b a different ESR signal emerged in some samples of the series. When rerun at 77°K, the P_a center[1] at $g = 1.999$ appeared in the n-doped wafers, with largest amplitude for 25 Ω cm. Representative spectra are shown in Fig. 11. Its presence only in n-doped samples strongly suggests donor and/or conduction electrons. Simple etching tests with HF and HF-HNO_3 indicate that the observed signal does not arise from centers in the oxide, but rather from the first few micrometers of silicon beneath the interface. Unexpectedly large interface phosphorus accumulation in other samples has been observed by Auger spectroscopy.[13]

F. Concluding remarks

Interface states and ESR centers have been examined in oxidized silicon wafers prepared by a variety of semiconductor processing techniques. During the earlier part of this program, the observations indicated a relationship between the interface state density in non-H_2 annealed (111) samples and ESR signals with the concentration of spin centers approximately equal to D_{it}. Both P_b and D_{it} were found to be greatly reduced by steam oxidations and hydrogen annealing. Both P_b and D_{it} were also regenerated by extended N_2 anneals at 500°C. In the present study, (100) wafers were included. For (111) and (100) wafers the proportionality of D_{it} and P_b was generally maintained throughout a wide variation in processing methods and over a limited range of n- and p-doping level. Nonetheless, some possibly significant differences between the response of n- and p-doped silicon to nitrogen anneals have been observed, which cannot be explained satisfactorily at this time.

A major objective of this study was the assessment of the value of ESR in studies of the Si/SiO_2 interface and its possible contribution to our knowledge of interface states. Despite the occurrence of numerous tempting correlations, there are considerations which make it difficult to establish a broad and conclusive relationship between P_b and D_{it} for diverse physical and chemical situations at this time. As an example of the problem, a different type of interface states (donor- or acceptor-like) seems to arise from different processing conditions. Nitrogen and argon anneal/cool create both types of states, whereas oxygen-cooled samples are characterized by predominantly donor states in the lower portion of the bandgap. How the nature of the states relates

to the ESR signal is not presently clear. Very carefully controlled series of H_2 and N_2 anneals, with close monitoring of P_b level and D_{it} distribution, are suggested. In another concern, values of D_{it} are observed with some potential applied to the interface, while ESR values are measured in a "no-bias" condition. Application of a surface potential during the ESR measurement may result in different levels of P_b signals. Nonetheless, the observation of the widespread correlation between the ESR P_b signal and midgap interface state density is an important result of this investigation. In consideration of the reasonable crystallographic picture suggested by ESR, it seems a useful characterization tool for further studies on the electrical and structural features of the Si/SiO_2 interface.

ACKNOWLEDGEMENTS

The authors would like to thank Julia Bien and Edward Dovichi for portions of the experimental work, and Dr. J. M. Early for support and helpful suggestions. This work has been partially sponsored by ARO Contract No. DAAG 29-78-C-0033.

Accession For
NTIS GRA&I ☒
DTIC TAB ☐
Unannounced ☐
Justification
By
Distribution/
Availability Codes
Dist | Avail and/or Special
A | 21

DTIC COPY INSPECTED

[1] B. E. Deal, in *Semiconductor Silicon* 1977, edited by H. R. Huff, and E. Sirtl (Electrochemical Soc., Princeton, N. J., 1977), p. 276.
[2] P. J. Caplan, E. H. Poindexter, B. E. Deal, and R. R. Razouk, J. Appl. Phys. **50**, 5847 (1979).
[3] Y. Nishi, Jpn. J. Appl. Phys. **10**, 52 (1971).
[4] B. E. Deal, J. Electrochem. Soc. **127**, 979 (1980). In the present paper, recommended new symbols for oxide charges will be used: D_{it} interface trap density, units $cm^{-2}eV^{-1}$ (formerly N_{ss}, N_{st}, N_{it}; interface state density, surface state density, fast state density); N_f, number of fixed oxide charges per units cm^{-2} (formerly Q_{ss}/q, Q_{ss}/q, *et al.*).
[5] M.F. Chung and D. Haneman, J. Appl. Phys. **37**,1879 (1966).
[6] D. L. Griscom, E. J. Freibele, and G H. Sigel, Jr., Solid State Commun. **15**, 479 (1974).
[7] E. G. Sieverts, Doctoral dissertation, University of Amsterdam, 1978 (unpublished).
[8] D. L. Griscom, in *The Physics of SiO_2 and its Interfaces*, edited by S. T. Pantelides (Pergamon, New York, 1978), p. 232.
[9] A. Goetzberger, E. Klausmann, and M. J. Schulz, CRC Crit. Rev. Solid State Sci. **6**, 1 (1976).
[10] R. R. Razouk and B. E. Deal, J. Electrochem. Soc. **126**, 1574 (1979).
[11] S. I. Raider, R. A. Gdula, and J. R. Petrak, Appl. Phys. Lett. **27**,150 (1975).
[12] E. Kooi, J. G. van Lierop, and J. A. Appels, J. Electrochem. Soc. **123**, 117 (1976).
[13] S. A. Schwarz, C. R. Helms, W. E. Spicer, and N. J. Taylor, J. Vac. Sci. Technol. **15**, 227 (1978).